Dopamine tone regulates D1 receptor trafficking and delivery in striatal neurons in dopamine transporter-deficient mice

Brigitte Dumartin*, Mohamed Jaber*, Francois Gonon*, Marc G. Caron†, Bruno Giros‡, and Bertrand Bloch*§

*Laboratoire d'Histologie-Embryologie, Unite Mixte de Recherche Centre National de la Recherche Scientifique 5541, Interactions Neuronales et Comportements, Université V. Ségalen, 146 Rue Léo-Saignat, 33076 Bordeaux Cedex, France; †Howard Hughes Medical Institute Laboratories, Departments of Cell Biology and Medicine, Duke University Medical Center, Durham, NC 27710; and ‡Unité Institut National de la Sante et de la Recherche Medicale 513, Faculté de Médecine, 8 Avenue du Général Sarrail, 94010 Créteil Cedex, France.

Edited by Tomas Hökfelt, Karolinska Institute, Stockholm, Sweden, and approved November 4, 1999 (received for review August 11, 1999)

***In vivo*, G protein-coupled receptors (GPCR) for neurotransmitters undergo complex intracellular trafficking that contribute to regulate their abundance at the cell surface. Here, we report a previously undescribed alteration in the subcellular localization of D1 dopamine receptor (D1R) that occurs *in vivo* in striatal dopaminoceptive neurons in response to chronic and constitutive hyperdopaminergia. Indeed, in mice lacking the dopamine transporter, D1R is in abnormally low abundance at the plasma membrane of cell bodies and dendrites and is largely accumulated in rough endoplasmic reticulum and Golgi apparatus. Decrease of striatal extracellular dopamine concentration with 6-hydroxydopamine (6-OHDA) in heterozygous mice restores delivery of the receptor from the cytoplasm to the plasma membrane in cell bodies. These results demonstrate that, *in vivo*, in the central nervous system, the storage in cytoplasmic compartments involved in synthesis and the membrane delivery contribute to regulate GPCR availability and abundance at the surface of the neurons under control of the neurotransmitter tone. Such regulation may contribute to modulate receptivity of neurons to their endogenous ligands and related exogenous drugs.**

Most neurotransmitters act through membrane-bound G protein-coupled receptors (GPCR) (1, 2). These receptors are synthesized in the cytoplasm and, in most instances, delivered at the plasma membrane of cell bodies and dendrites (3–6). They frequently display extrasynaptic localization (3–8). In the central nervous system, activation of these receptors in acute conditions, through the release of their endogenous ligand, such as substance P or dopamine, or through injection of exogenous agonists, leads within minutes to modifications of their trafficking and subcellular localization (8–14). These modifications include mainly the translocation of the receptor from the surface of the neurons to the endosomal compartment in the cytoplasm, leading within minutes to decreased receptor abundance at the membrane. *In vivo* and *in vitro* experiments have shown that internalization under acute stimulation leads to receptor recycling at the membrane within minutes to a few hours after the end of agonist action (8–15). *In vitro* studies have demonstrated that internalization in the cytoplasm is associated with molecular modifications of the receptors that ultimately lead to their desensitization, down-regulation, and recycling (15–17). A major role of the cellular trafficking of GPCR after acute stimulation is to contribute to the reestablishment of the cellular responsiveness (16). However, because different GPCR appear to recycle with markedly different time courses (17), such alterations of subcellular compartmentalization may contribute to regulate sensitivity of neurons to neurotransmitters or drugs through the control of receptor availability and abundance at the surface of neurons.

We recently demonstrated that the D1 dopamine receptor (D1R) undergoes such internalization in endosomes and recycling at the membrane in striatal neurons under acute activation by D1R agonist or amphetamine (12). Here, we provide evidence that chronic stimulation of D1R is associated with other modes of alteration of D1R localization, including exaggerated accumulation of the receptor in the cytoplasmic compartments involved in synthesis. For this, we used mice with a deletion for the dopamine transporter (DAT) gene, which display chronic hyperdopaminergic tone including high extracellular dopamine concentration in the striatum. These mice were shown to down-regulate D1R (18, 19). By using immunohistochemical analysis at the cellular and ultrastructural level, we demonstrate that in knockout ($DAT^{-/-}$) mice, the receptor accumulates in rough endoplasmic reticulum and Golgi apparatus and is greatly lowered at the plasma membrane in dendrites and cell bodies. These properties are also evident, albeit less pronounced, in heterozygous ($DAT^{+/-}$) mice. Decreasing extracellular dopamine concentration with 6-hydroxydopamine (6-OHDA) in $DAT^{+/-}$ mice provokes recruitment of the D1R to the plasma membrane of cell bodies with concomitant decrease in the endoplasmic reticulum, therefore suggesting that membrane delivery of the receptor from the cytoplasm is a regulated mechanism.

Methods

Knockout Mice. The mouse strain in which the gene encoding the DAT has been disrupted was obtained by *in vivo* homologous recombination as described previously (18). Wild-type mice ($DAT^{+/+}$), heterozygous mice ($DAT^{+/-}$), and homozygous mice ($DAT^{-/-}$) between the ages of 2–4 mo were used. They were maintained under standard housing conditions in the transgenic animal facility at the Université Victor Segalen, and given food and water ad libitum. Experiments were performed in accordance with the guidelines of the French Agriculture and Forestry Ministry (decree 87849, license 01499) and with the approval of the Centre National de la Recherche Scientifique.

6-OHDA Injections in the Medial Forebrain Bundle (MFB) of $DAT^{+/-}$ Mice for D1R Detection. Injections were performed in the MFB as described previously in rat (20). Briefly, adult $DAT^{+/-}$ mice were anesthetized with chloral hydrate (400 mg/kg) and fixed on a stereotaxic frame with a mouse adaptator (Stoelting) according to Franklin and Paxinos's atlas. Dopaminergic axons into MFB were localized with a carbon fiber electrode, which monitored the extracellular 3,4-dihydroxyphenylacetic acid (DOPAC) (20). This electrode was implanted 1.05 mm lateral to

This paper was submitted directly (Track II) to the PNAS office.

Abbreviations: GPCR, G protein-coupled receptor; D1R, D1 dopamine receptor; DAT, dopamine transporter; MFB, medial forebrain bundle; DOPAC, 3,4-dihydroxyphenylacetic acid; 6-OHDA, 6-hydroxydopamine.

§To whom reprint requests should be addressed. E-mail: bertrand.bloch@u-bordeaux2.fr.

The publication costs of this article were defrayed in part by page charge payment. This article must therefore be hereby marked "*advertisement*" in accordance with 18 U.S.C. §1734 solely to indicate this fact.

the medial line and 2.1 mm posterior to bregma. When the depth corresponding to the maximal amplitude of the DOPAC signal was determined, the carbon fiber electrode was replaced by a glass micropipette filled with the following solution: 9 g/liter NaCl/0.2 g/liter KCl/1 mM $CaCl_2 \cdot 2H_2O$/1 mM ascorbic acid/3 μg/μl 6-OHDA (Sigma). Using an air pressure system, three injections (220 nl in 1 min each) were performed at different vertical levels: 0.3 mm above, at the level of, and 0.3 mm below the point where the DOPAC signal reached its maximum. Animals were sacrificed 3 days after 6-OHDA injection for immunohistochemical studies.

Electrochemical Monitoring of Extracellular Dopamine Level. In an independent experiment, the localization of the MFB was electrochemically determined as described, and heterozygous mice were treated with pargyline (75 mg/kg, i.p.) to block dopamine degradation. One hour later, an electrochemically treated carbon fiber electrode was implanted in the striatum at the following coordinates: 1.6 mm lateral to medial line, 1.0 mm rostral to bregma, and 2.75 mm below the cortical surface. Voltammograms from −240 mV to +200 mV were recorded every 90 s with differential normal pulse voltammetry and showed a catechol peak appearing at +90 mV. Because DOPAC synthesis was blocked by pargyline, this catechol peak entirely corresponded to extracellular dopamine (20). After a control period of 15 min, 6-OHDA or vehicle were injected in the MFB as described above, and catechol peak was continuously monitored.

Immunohistochemical Detection of D1R. D1R was detected with a polyclonal D1R antibody produced as described (21). The specificity of the antiserum and immunolabelings were previously demonstrated (6, 12, 21).

Fixation and processing for immunohistochemistry were conducted as previously described (12) for rats with minor modifications listed below. Mice were anesthetized with chloral hydrate, intracardially injected with 0.2 ml of heparin (Choay Laboratories, Paris) and perfused with 20 ml of 0.9% NaCl and 100 ml of fixative [2% paraformaldehyde and 0.1% glutaralde-

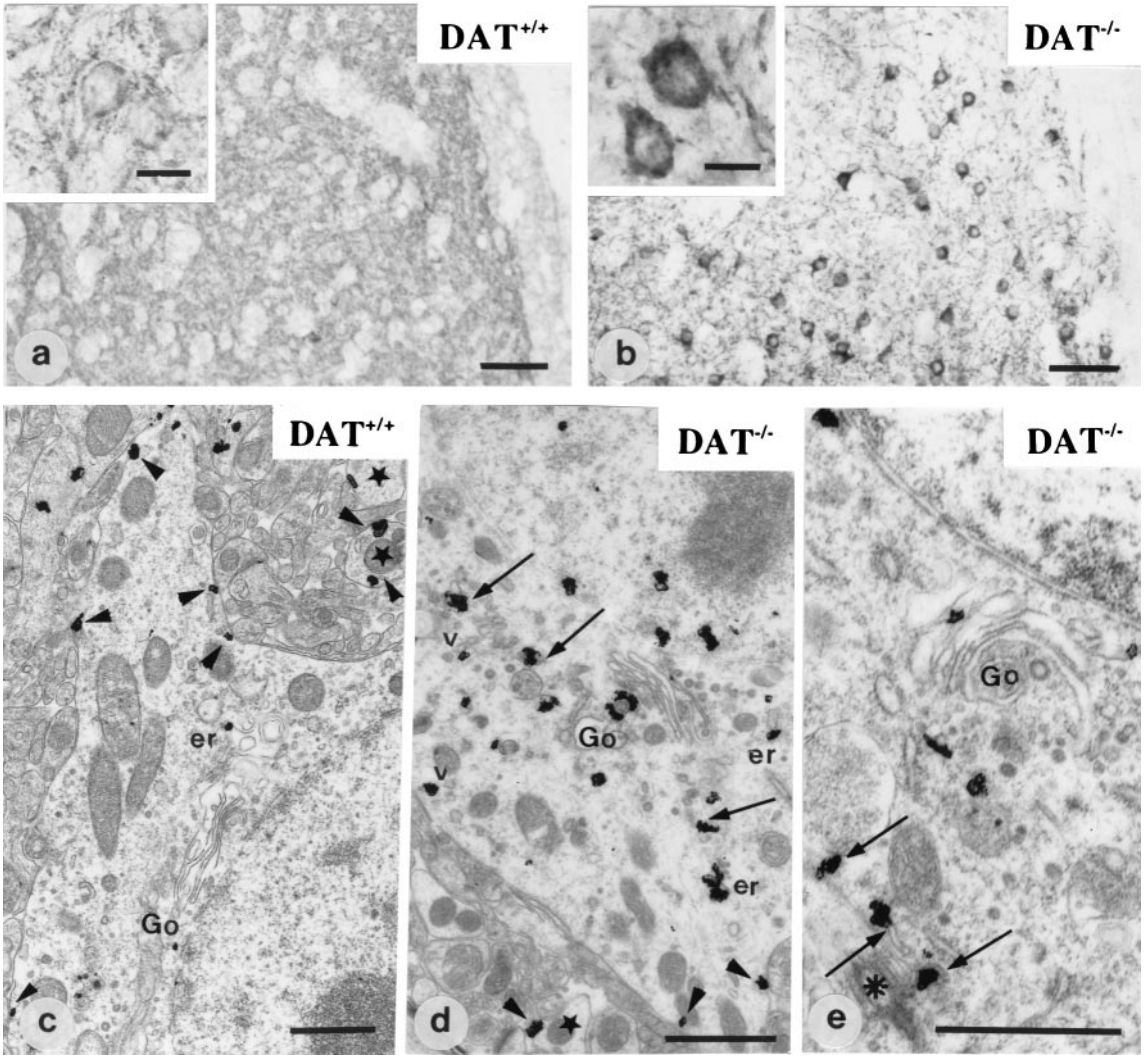

Fig. 1. Immunohistochemical detection of D1R at the light and electron microscopic level in $DAT^{+/+}$ (*a* and *c*) and $DAT^{-/-}$ mice (*b*, *d*, and *e*). In wild-type mice ($DAT^{+/+}$) (*a* and *c*), D1R is located in the neuropile and at the plasma membrane of cell bodies (*a*, *Inset*; and *c*, arrowheads). Stars point to dendrite profiles. Ultrastructural localization of D1R in *c* shows very few intracytoplasmic immunoparticles associated with the Golgi apparatus (Go) and the endoplasmic reticulum (er). In $DAT^{-/-}$ mice (*b*, *d*, and *e*), D1R is located primarily in the cytoplasm of cell bodies (*b*, *Inset*). The receptor is associated with the Golgi apparatus (Go), the endoplasmic reticulum (arrows and er), and some vesicles (v). A few immunoparticles are detected along the plasma membrane (*d*, arrowheads). In *e*, part of D1R immunoreactivity associated with endoplasmic reticulum (arrows) is in the pericentriolar area (asterisk). [Scale bar = 50 μm (*a* and *b*), 10 μm (*a* and *b*, *Insets*), and 1 μm (*c*, *d*, and *e*)].

hyde in 0.1 M phosphate buffer (pH 7.4)]. Brains were removed, left in 2% paraformaldehyde overnight, and cut with a Vibratome. Sections were cryoprotected, freeze-thawed, and preincubated in 0.2% PBS containing acetylated BSA (BSAc) for 1 h.

Detection of D1R on Vibratome Sections with Tyramide Signal Amplification. Vibratome sections were incubated in D1R antiserum (1/10,000) for 48 h at 4°C, incubated in biotinylated goat anti-rabbit IgG (1/200 in PBS-BSAc; Amersham Pharmacia) for 2 h, then in streptavidin-horseradish peroxidase (SA-HRP) for 30 min (1/100). They were washed and incubated in biotinyl tyramide. After washing, the sections were incubated again in SA-HRP (1/100) for 30 min and rinsed. Peroxidase activity was revealed with 3,3′-diaminobenzidine in the presence of hydrogen peroxide, and the sections were mounted for observation at the light microscopic level.

Detection of D1R by Immunogold Method at the Ultrastructural Level. Vibratome sections were incubated with D1R antibody at a dilution of 1/1,000, rinsed in PBS-BSAc with gelatin, and incubated in goat anti-rabbit IgG conjugated to ultrasmall colloidal gold particles (0.8 nm; Aurion, the Netherlands). After several washes, the sections were postfixed in 1% glutaraldehyde for 10 min and rinsed (two times in PBS and two times in 2% sodium acetate). The gold labeling was intensified by using a silver enhancement kit (Aurion). The sections were rinsed and postfixed in osmium tetroxide. After washing, they were dehydrated in ascending series of dilution of ethanol, including 70% ethanol containing 1% uranyl acetate. They were then treated with propylene oxide (two times for10 min), impregnated in resin overnight (Durcupan ACM; Fluka), mounted on glass slides, and curred at 60°C for 48 h. Areas of interest were cut out from the sections and glued to blank cylinders of resin. Ultrathin sections were collected on copper grids, contrasted with lead citrate, and observed in a Philips CM10 electron microscope.

Quantitative Analysis of the D1R Distribution. Morphometric analysis was performed at the electron microscopic level from immunogold-treated sections. Photomicrographs were collected, and the negatives were scanned (Magicscan, UMax) and analyzed with METAMORPH software (Universal Corporation, Paris). Gold particles were identified and counted either in association with plasma membrane or with intracytoplasmic compartments. Three morphologically defined subcellular compartments were counted in the cell bodies: Golgi apparatus, rough endoplasmic reticulum, and vesicles. Immunoparticles were classified as associated with an unidentified compartment when they were associated with cytoplasmic structures that could not be identified. Comparative analysis was performed on sections from four $DAT^{-/-}$ mice, four $DAT^{+/+}$ mice, and six $DAT^{+/-}$ mice (15 cell bodies and 20–30 dendritic profiles per animal). Four unilaterally 6-OHDA-injected mice were analyzed. Injected side was compared with the control contralateral side. The results were expressed as a number of immunoparticles per membrane length (100 μm) and cytoplasmic surface (100 μm^2). For each set of experiments, the values were subjected to a one-way ANOVA followed by a post hoc *t* test.

Results

Localization of D1R Immunoreactivity in the Striatal Neurons of Wild-Type ($DAT^{+/+}$) Mice. Analysis at the light microscopic level demonstrated D1R immunoreactivity throughout the striatum with prominent labeling of the neuropile and of the membrane of the cell bodies (Fig. 1*a*). Ultrastructural studies confirmed that immunostained structures were medium-sized spiny neurons and that a large part of immunogold particles corresponding to D1R were located at the plasma membrane of perikarya and dendrites (Fig. 1*c*), as previously shown in normal adult rat (3, 6, 12). In the cell body cytoplasm, D1R immunoreactivity was present in several compartments, including mostly the rough endoplasmic reticulum (54% of cytoplasmic immunoreactivity), Golgi apparatus (20%), and vesicles (17.5%). A small percentage of immunoreactivity (8.5%) was not associated with a recognizable organelle (Fig. 2).

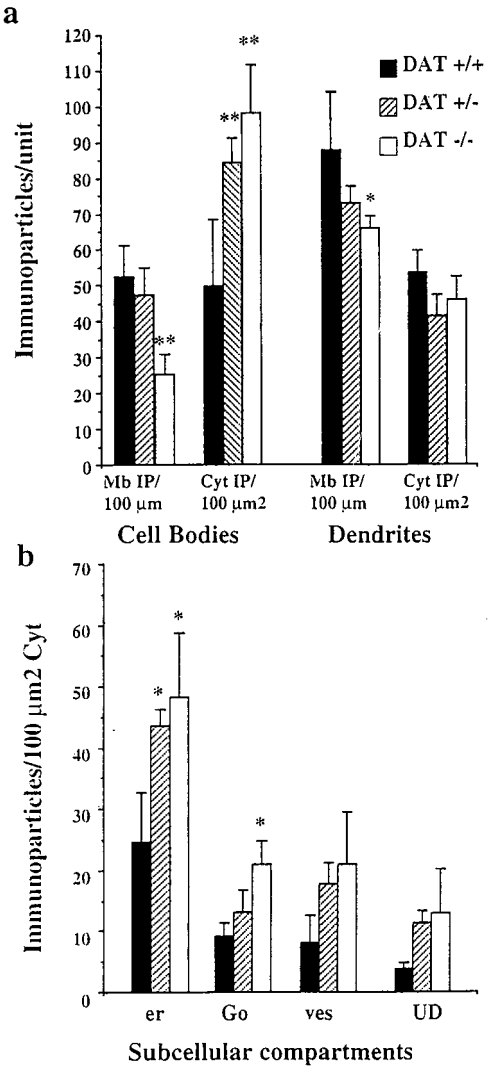

Fig. 2. Quantitative analysis of the subcellular distribution of D1R at the electron microscopic level. (*a*) Measure of D1R immunoreactivity at the plasma membrane and in the cytoplasm: The number of immunoparticles +/− SEM was counted in relation to the plasma membrane length (Mb IP/100 μm) and to the cytoplasmic surface (Cyt IP/100 μm^2) in cell bodies and dendrites. $DAT^{-/-}$ neurons show a sharp and significant decrease of D1R at the plasma membrane of cell bodies and dendrites as compared with $DAT^{+/+}$ neurons. They also display sharp increase of intracytoplasmic immunoparticles in the cell bodies. $DAT^{+/-}$ mice display significant increase of D1R in the cytoplasm without significant reduction at the plasma membrane. (*b*) Measure of D1R immunoreactivity in the cytoplasmic organelles in the cell bodies. In $DAT^{+/+}$ cell bodies, the largest part of cytoplasmic D1R is detected in association with the endoplasmic reticulum (er) and the Golgi apparatus (Go). Other particles are present in vesicles (ves) or in an unidentified cytoplasmic compartment (UD). Immunoparticles density is dramatically increased in the endoplasmic reticulum and in the Golgi apparatus in $DAT^{-/-}$ mice and only in the endoplasmic reticulum in $DAT^{+/-}$ mice. **, $P \leq 0.01$; *, $P < 0.05$.

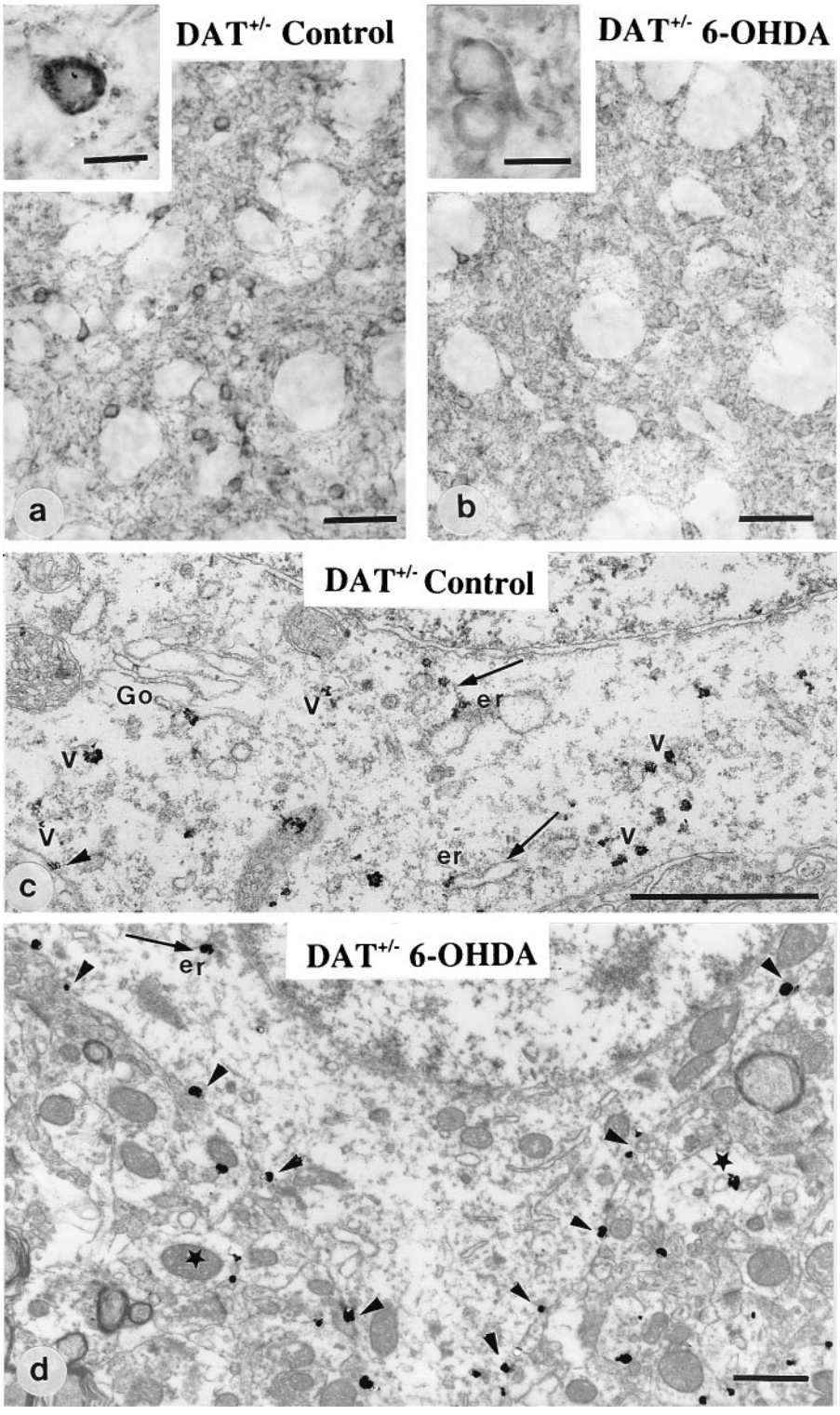

Fig. 3. Immunohistochemical detection of D1R at the light and electron microscopic level in heterozygous mice unilaterally treated with 6–0HDA. In the control side (*a* and *c*), striatal neurons display D1R mostly located in the cytoplasm, associated with the Golgi apparatus (Go), the endoplasmic reticulum (er), and vesicles (arrows). In the 6-OHDA-injected side (*b* and *d*), D1R appears homogeneously distributed in the neuropile and largely redistributed at the plasma membrane of cell bodies (*b*, *Inset*; and *d*, arrowheads) with a limited number of immunoparticles in the cytoplasm. Star points to a dendritic profile. (Magnification bar: *a* and *b* = 50 μm; *a* and *b*, *Insets* = 10 μm; *c* and *d* = 1 μm).

Localization of D1R Immunoreactivity in Mice with Inactivated DAT Gene. $DAT^{-/-}$ mice demonstrated dramatic alterations of D1R subcellular localization in neurons. Analysis of D1R distribution at the light microscopic level showed that the cell bodies displayed intense intracytoplasmic labeling (Fig. 1*b*). Observation (Fig. 1 *d* and *e*) and quantification (Fig. 2) at the ultrastructural level demonstrated a significant decrease of D1R immunoparticles at the plasma membrane of cell bodies and dendrites

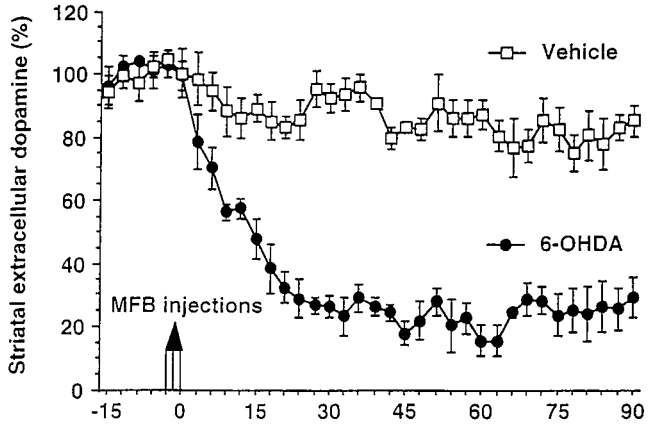

Fig. 4. Effect of 6-OHDA injection in the MFB on the extracellular dopamine concentration in the striatum of DAT$^{+/-}$ mice. The extracellular dopamine concentration was monitored every 90 s in the striatum with an electrochemically treated carbon fiber electrode combined with differential pulse voltammetry. Injections of the 6-OHDA solution or of the vehicle were performed after a control period of 15 min. The extracellular dopamine level was expressed in percent of the mean of the 10 absolute peak amplitudes recorded before injections. 6–0HDA provokes a rapid and dramatic decrease of the dopamine content as compared with control experiment with vehicle.

(−52% and −40%, respectively, as compared with DAT$^{+/+}$ mice). This was associated with an increase of D1R immunoparticles in the cytoplasm of cell bodies as compared with DAT$^{+/+}$ mice (+97%), with D1R immunoreactivity preferentially concentrated in the perinuclear area. Analysis of cytoplasmic compartments demonstrated that the increased immunoreactivity was prominent and significant in the endoplasmic reticulum and Golgi apparatus (+95% and +131%, respectively). D1R abundance or distribution was not modified in dendrite cytoplasm.

Localization of D1R Immunoreactivity in Heterozygous Mice: Effect of 6-OHDA. DAT$^{+/-}$ mice displayed alterations of D1R intermediate between DAT$^{+/+}$ and DAT$^{-/-}$ mice with large variations from one animal to another (Fig. 3 *a* and *c*). In DAT$^{+/-}$ mice with significant increase in cytoplasmic D1R immunoreactivity, striatal neurons were analyzed after decrease of extracellular dopamine concentration provoked by a unilateral injection of 6-OHDA in the MFB (Fig. 4) as previously developed (20). Indeed, since 6-OHDA acts by entering in dopamine neurons through the DAT molecule, DAT$^{-/-}$ mice could not be used in such experiments to obtain low dopamine level in the striatum. Three days after injection, 6-OHDA-injected side of DAT$^{+/-}$ mice showed prominent changes in D1R immunoreactivity as compared with the control contralateral striatum of the same animal (Fig. 3 *b* and *d* and Fig. 5). The control side displayed D1R prominently in the cytoplasm of cell bodies, associated with Golgi complex, endoplasmic reticulum, and vesicles (Fig. 3*c*). 6-OHDA-injected side showed redistribution of D1R immunoreactivity at the plasma membrane of the cell bodies (Fig. 3 *b* and *d*). Quantification at the ultrastructural level (Fig. 5) confirmed increased D1R immunoreactivity at the plasma membrane of cell bodies in 6-OHDA-injected side (+54% as compared with control side) with concomitant decrease of D1R immunoreactivity in the cytoplasm of cell bodies (−32% as compared with the control side). Decrease was significant in the rough endoplasmic reticulum and the vesicular compartment (−33% and −55%, respectively). Dendrites did not show changes in membrane-bound D1R immunoreactivity, but showed increased intracytoplasmic immunoreactivity (+81%).

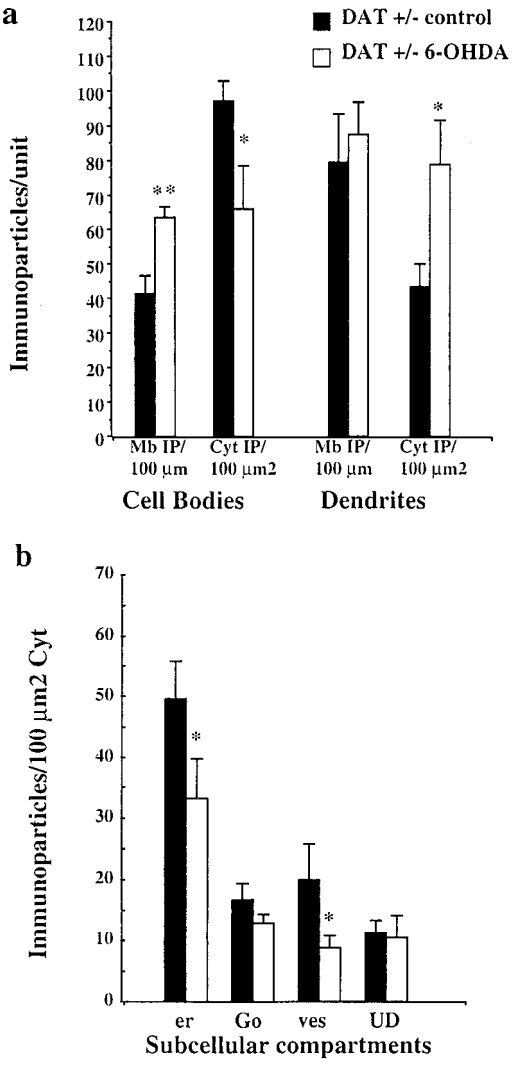

Fig. 5. Quantitative analysis of the subcellular distribution of D1R in DAT$^{+/-}$ mice after 6-OHDA injection. (*a*) Measure of D1R immunoreactivity at the plasma membrane and in the cytoplasm: The number of immunoparticles +/− SEM was counted in relation to the plasma membrane length (Mb IP/100 μm) and to the cytoplasmic surface (Cyt IP/100 μm^2) in cell bodies and dendrites. Cell bodies in 6-OHDA-injected side display decreased cytoplasmic D1R and increased D1R at the plasma membrane. Dendrites display unchanged membrane-bound receptor but increased cytoplasmic D1R. (*b*) Measure of D1R immunoreactivity in the cytoplasmic organelles in the cell bodies: the endoplasmic reticulum (er) and the vesicles (ves) display a significant decrease of D1R in 6-OHDA-injected side as compared with the control side. **, $P \leq 0.001$; *, $P \leq 0.05$.

Discussion

Modifications of abundance and availability of GPCR at the surface of the neurons contribute to regulate sensitivity to neurotransmitters (15). Changes in subcellular localization of these receptors and internalization in endosomes after acute stimulation have recently been shown to contribute to these modifications (8–14).

In the present study, we have analyzed the subcellular localization of D1R in neurons under chronic stimulation by dopamine in mice that display neurochemical and behavioral features of exaggerated dopamine tone, including high extracellular dopamine concentration in the striatum. In these animals, D1R is down-regulated in the striatal dopaminoceptive neurons at the mRNA and protein levels (ref. 15, and unpublished observa-

tions). Such down-regulation most probably reflects an adaptive response of the striatal neurons to high dopamine concentration. We show here that this regulation involves D1R sequestration in cytoplasmic compartments, which can be partially reversed by decrease of the dopamine tone.

Indeed, not only D1R displays decreased abundance at the plasma membrane in cell bodies and in dendrites, but also this decrease is associated with exaggerated receptor abundance specifically in the two cytoplasmic compartments that contribute to synthesis, namely the endoplasmic reticulum and the Golgi apparatus, where D1R is not available for ligands. The most conservative explanation of these results is to consider that, under conditions of down-regulation, the D1R, once synthesized, remains trapped in these cytoplasmic compartments and is not delivered to the plasma membrane. This phenomenon is reversible because recruitment of D1R to the plasma membrane of cell bodies and decrease of the immunoreactivity in the endoplasmic reticulum is observed after decrease of extracellular dopamine concentration with 6-OHDA treatment. This suggests that, in such conditions, dopamine decrease in the striatum constitutes a signal for delivery of D1R at the plasma membrane. 6-OHDA injection had no effect on D1R abundance at the membrane of dendrites, and increased immunoreactivity in their cytoplasm. A delayed membrane delivery of D1R in dendrites resulting from the intraneuronal transport of the receptors from the cell body to the dendrites after dopamine decrease may explain such discrepancy. This hypothesis would explain the increased intradendritic D1R immunoreactivity after 6-OHDA. Differential innervation of cell bodies and dendrites by dopamine fibers (22) may possibly lead to heterogenous decrease of dopamine concentrations at the vicinity of cell bodies and dendrites.

Receptor abundance at the plasma membrane is determined by the activity of several pathways of receptor trafficking. These include the delivery of newly synthesized receptor, receptor internalization after activation, receptor degradation in lysosomes, and receptor recycling at the membrane (14, 15). Modifications of GPCR trafficking after acute stimulation that include internalization in endosomes and receptor recycling at the membrane within a few hours have been substantially documented (8–15). The sequestration of GPCR in the rough endoplasmic reticulum and Golgi apparatus may be a previously underestimated mechanism controlling receptor abundance at the surface of the neurons under situation of chronic stimulation. However, we cannot exclude that down-regulation of the D1R may also include degradation or accelerated endocytosis, but the absence of variation in endosomal or lysosomal structures bearing D1R immunoreactivity in the cytoplasm of neurons of $DAT^{-/-}$ mice does not favor this hypothesis.

There is limited information on the functional importance of delivery to the membrane of newly synthesized receptors under chronic activation. *In vivo*, GPCR are generally located at the plasma membrane of neurons, but can also be found prominently in the cytoplasm, especially under high neurotransmitter tone (7). Indeed, anatomical evidence suggests that in the normal brain, a given GPCR may be present in the cytoplasm or at the plasma membrane, depending on the relationships between the innervation delivering the ligand and the neurons bearing receptors, as shown for somatostatin (7) or acetylcholine receptor (23). Also, *in vitro* models demonstrate that acute dopamine agonist treatment can promote the delivery of newly synthesized receptors from an unidentified cytosolic compartment to the plasma membrane of renal cells (24). Long-term exposure to cocaine that blocks dopamine transporter activity down-regulates D1R in striatal neurons (25). These findings raise the interesting question as to whether chronic alteration of dopamine transporter production or action as observed during aging or psychostimulant administration (25–27) may also influence D1R trafficking and delivery in certain pathological situations. At any rate, the present results provide evidence that regulated delivery of GPCR from the endoplasmic reticulum and Golgi complex to the plasma membrane can be a component of the response of neurons to abnormal stimulation by a neurotransmitter. It can be expected that such phenomenon contributes to the control of the abundance of GPCR available for ligand at the surface of the neurons and consequently of signaling efficiency.

We thank C. Vidauporte for excellent artwork, F. Georges for expert help in statistical analysis, and M. C. Fournier for expert technical assistance. We also thank the members of the SERCOMI and the members of transgenic facilities at the University V. Ségalen. We thank Association France Parkinson for efficient financial support.

1. Hoyer, D. & Humphrey, P. P. (1997) *J. Recept. Signal Transduct. Res.* **17,** 551–568.
2. Sokoloff, P. & Schwartz, J. C. (1995) *Trends Pharmacol. Sci.* **16,** 270–274.
3. Hersch, S. M., Ciliax, B. J., Guterkunst, C. A., Rees, H. D., Heilman, C. J., Yung, K. K., Bolam, J. P., Ince, E., Yi, H. & Levey, A. I. (1994) *J. Neurosci.* **14,** 3351–3363.
4. Liu, H., Brown, J. L., Jasmin, L., Maggio, J. E., Vigna, S. R., Mantyh, P. W. & Basbaum, A. I. (1994) *Proc. Natl. Acad. Sci. USA* **91,** 1009–1013.
5. Levey, A. I., Edmunds, S. M., Hersch, S. M., Wiley, R. G. & Heilman, C. J. (1995) *J. Comp. Neurol.* **351,** 339–356.
6. Caillé, I., Dumartin, B. & Bloch, B. (1996) *Brain Res.* **730,** 17–31.
7. Dournaud, P., Boudin, H., Schonbrunn, A., Tannenbaum, G. S.& Beaudet, A. (1998) *J. Neurosci.* **18,** 1056–1071.
8. Mantyh, P. W., Allen, C. J., Ghilardi, J. R., Rogers, S. D., Mantyh, C. R., Liu, H. T., Basbaum, A. I., Vigna, S. R. & Maggio, J. E (1995) *Proc. Natl. Acad. Sci. USA* **92,** 2622–2626.
9. Mantyh, P. W., DeMaster, E., Malhotra, A., Ghilardi, J. R., Rogers, S. D., Mantyh, C. R., Liu, H. T., Basbaum, A. I., Vigna, S. R. & Maggio, J. E. (1995) *Science* **268,** 1629–1632.
10. Faure, M. P., Alonzo, A., Nouel, D., Gaudriault, G., Dennis, M., Vincent, J. P. & Beaudet, A. (1995) *J. Neurosci.* **15,** 4140–4147.
11. Sternini, C., Spann, M., Anton, B., Keith, D. E., Jr., Bunnet, N. W., von Zastrow, M., Evans, C. & Brecha, N. C. (1996) *Proc. Natl. Acad. Sci. USA* **93,** 9241–9246.
12. Dumartin, B., Caillé, I., Gonon, F. & Bloch, B. (1998) *J. Neurosci.* **18,** 1650–1661.
13. Bernard, V., Laribi, O., Levey, A. I. & Bloch, B. (1998) *J. Neurosci.* **18,** 10207–10218.
14. Bloch, B., Dumartin, B. & Bernard, V. (1999) *Trends Pharmacol. Sci.* **20,** 315–319.
15. Koenig, J. A. & Edwardson, M. J. (1997) *Trends Pharmacol. Sci.* **18,** 276–287.
16. Ferguson, S., Barak, L., Zhang, J. & Caron, M. (1996) *Can. J. Physiol. Pharmacol.* **721,** 1095–1110.
17. Zhang, J., Barak, L., Anborgh, P., Laposte, S., Caron, M. & Ferguson, S. (1999) *J. Biol. Chem.* **274,** 10999–11006.
18. Giros, B., Jaber, M., Jones, S. R., Wightman, R. M. & Caron, M. G. (1996) *Nature (London)* **379,** 606–612.
19. Jones, S. R., Gainetdinov, R. R., Jaber, M., Giros, B. Wightman, R. M. & Caron, M. G. (1998) *Proc. Natl. Acad. Sci. USA* **95,** 4029–4034.
20. Svenningsson, P., Fourreau, L., Bloch, B., Fredholm, B. B., Gonon, F. & Le Moine, C. (1999) *Neuroscience* **89,** 827–837.
21. Caillé, I., Dumartin, B., Le Moine, C., Begueret, J. & Bloch, B. (1995) *Eur. J. Neurosci.* **7,** 714–722.
22. Groves, P. M., Linder, J. C. & Young, S. J. (1994) *Neuroscience* **58,** 593–604.
23. Bernard, V., Levey, A, & Bloch, B. (1999) *J. Neurosci.* **19,** 10237–10249.
24. Brismar, H., Asghar, M., Carey, R. M., Greengard, P. & Aperia, A. (1998) *Proc. Natl. Acad. Sci. USA* **95,** 5573–5578.
25. Moore, R., Vinsant, S., Nader, M. Porrino, L. & Friedman, D. P. (1999) *Synapse* **28,** 1–9.
26. Bannon, M. J., Poosch, M., Xia, Y., Goebel, D., Cassin, B. & Kapatos, G. (1992) *Proc. Natl. Acad. Sci. USA* **89,** 7095–7099.
27. Bannon, M. J. & Whitty, C. (1997) *Neurology* **48,** 969–977